Arch Orthop Trauma Surg (1999) 119:133–138

ORIGINAL ARTICLE

R. T. Müller · N. Schürmann

Shear strength of the cement metal interface – an experimental study

Received: 23 December 1996

Abstract The shear strength of the cement-metal interface using rods with different surface treatments and a clinical standardized cementing technique was studied. Under "dry" conditions, a low interface shear strength can be obtained with polished and smooth CoCrMo surfaces (peak-to-valley height R_t: 1 μm, average 0.2 MPa; 5 μm, 0.38 MPa). Grit-blasted and polymethylmethacrylate (PMMA)-precoated surfaces achieved higher values (PMMA precoat: average 5.16 MPa; CoCrMo peak-to-valley height R_t: 20 μm, average 8.61 MPa; 60 μm, average 7.8 MPa). After immersion in physiological saline solution for 60 days, the PMMA-precoated rods kept their initial stability whereas all the other test rods had lost their stability completely. A microscopic analysis of cross-sections revealed gap formations at the cement-metal interface to varying degrees (1–16 μm). PMMA-precoated rods rarely showed any gap formation at all. The above-mentioned gap formation was seen independently of the porosity at the cement-metal interface and corresponds to the clinical and postmortem observed debonding of the interface.

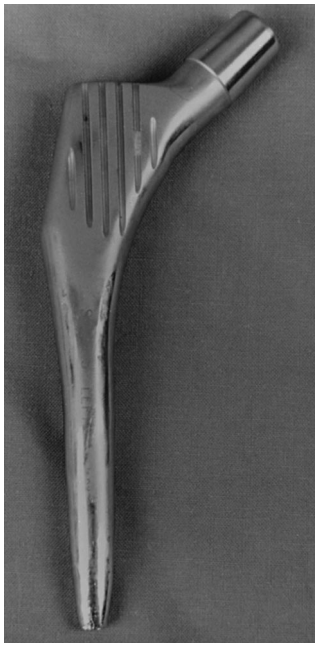

Fig. 1 Segmented polished stem of an originally matt prosthesis by micromovements after 5 years of in vivo function

Introduction

Radiological long-terms studies evaluating the cement-metal interface of cemented stems proved a debonding of the cement from the metal [15]. These results are stressed by the fact that some previously grit-blasted stems were polished in vivo by micromotions after debonding (Fig. 1). Postmortem examinations confirmed this debonding process which cannot be detected on X-rays during the first period after implantation [8]. Despite the interfacial debonding, patients remained painfree over many years due to a rotational stability provided by the implant design [15]. The absence of a rotational stability after debonding will enhance early loosening at the cement-metal interface as observed by Mohler et al. [14].

The loss of interfacial strength contributes to an increased wear at the cement-metal interface and permits distal migration of abraded particles. The debonding causes a stepwise subsidence of the implant in the cement mantle, thus reinforces the hoop strain in the cement mantle and consequently leads to an early failure of the cement mantle [12]. Depending on the implant material, massive abrasion and corrosion may occur, as observed on titanium alloys [20].

The rough surface of the cemented stems commonly implanted should allow a long-term bonding. Thus, the basic goal of this study was the determination of the shear strength that can be obtained by commonly used material surfaces under clinical working conditions.

R. T. Müller (✉) · N. Schürmann
Orthopädische Universitätsklinik, Hufelandstrasse 55,
D-45122 Essen, Germany
Fax: 0201-723-5910

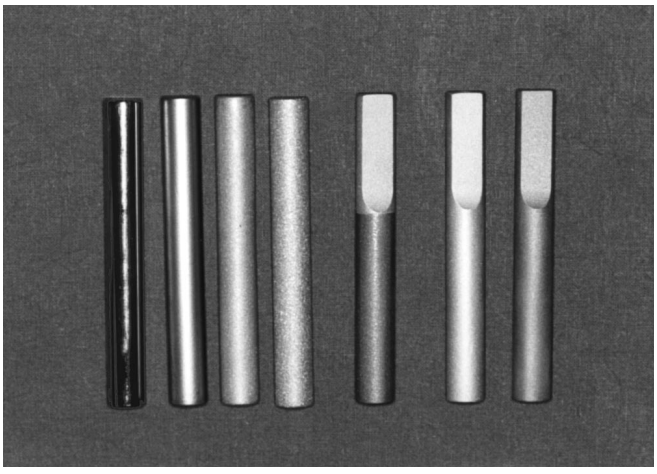

Fig. 2 Test rods used in this study (from *left* to *right*): CoCrMo (R_t: 1, 5, 20, 60 μm), CoCrMo-PMMA precoat (R_t: 27 μm) Ti-6A1-7Nb (R_t: 7, 12 μm)

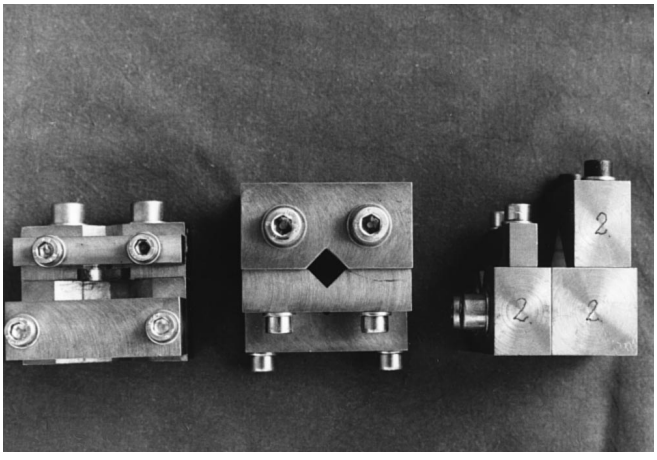

Fig. 3 Centring device for axial implantation of the rods in the tubes

Materials and methods

The experiments were performed with CoCrMo and Ti-6Al-7Nb alloys, both of them in clinical use for many years. The peak-to-valley height R_t is defined as the highest peak-to-valley height of the entire surface.

To analyse the dependence of the shear strength on the implant surface, CoCrMo rods with a roughness (R_t) of 1, 5, 20, and 60 μm were chosen. The surface roughness was produced by a corundum radiation method. The influence of a polymethylmethacrylate (PMMA) precoat on the shear strength was tested with CoCrMo-precoated rods. The peak-to-valley height R_t of the CoCrMo alloy was 27 μm with a PMMA layer thickness of 80 μm. The precoat layer was produced by spraying the PMMA powder onto the alloy and melting it on at 215° C.

In addition, we examined Ti-6Al-7Nb rods with two different standard implant surfaces, Ballotini 0.1–0.2 and Ballotini 0.1–0.2 + E440, commonly used for cementless implants. Ballotini are quartz glass balls which determine the surface finish, E 440 stands for precious corundum. The roughness (R_t) of the titanium rods was produced by a corundum radiation method. Due to the material characteristics, the implant surface roughness after corundum radiation differs between titanium and CoCrMo.

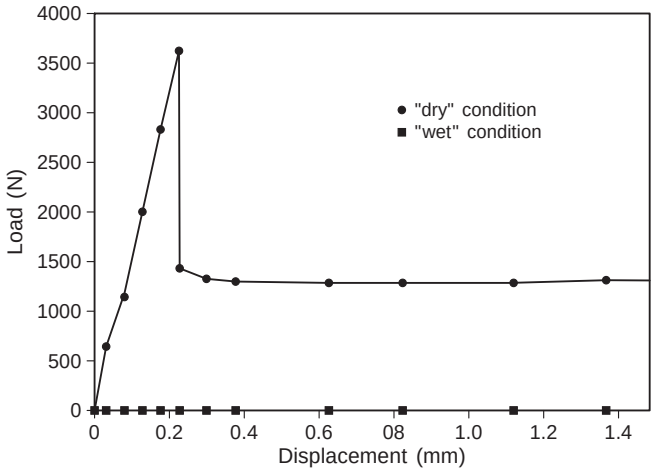

Fig. 4 Typical load-displacement curve using the example of a Ti-6Al-7Nb test rod (R_t 7 μm) under 'dry' (= room) and 'wet' (= physiological) conditions

All cylindrical rods, regardless of the implant material and surface, were 60 mm long and 10 mm wide. Figure 2 illustrates the test rods used.

The rods were inserted into polyvinylchloride (PVC) test-tubes (length 30 mm, inner diameter 22 mm, outer diameter 25 mm) with an inner continuous thread of 1 mm to guarantee a stable bond between cement and tube. To insert the rods axially into the tubes, three centring devices were used (Fig. 3).

The cement mantle thickness comprised 6 mm according to the Exeter stem system directives (cement mantle thickness of 2–6 mm, [6]). All test rods were used only once. One pack of bone cement (Palacos Merck 40.8 g) was sufficient for two surgeons to implant three rods in parallel.

The cementing technique was standardized in a manner that accurately represents current clinical practice. The cement components were prechilled at 4° C and mixed under vacuum (Merck vacuum system) for 45 s according to the manufacturer's instructions. Immediately afterwards, the bone cement was filled into a cement gun and pressurized until the end of the 4th min. Then the cement was filled axially into the test-tubes up to their proximal end with the cement gun, allowing air to leave distally. Afterwards, the tubes were inserted into the centring devices. The rods were implanted from proximal to distal, while the distal end of the tube was occluded. Thus, the cement had to squeeze out proximally. Finally, the screws of the centring device were tightened to ensure a stable position of the rod. The cement was allowed to harden for 20 min. The centricity of the centring device was checked regularly with a standard test specimen. The centricity of the rods was checked by a special testing device determining an exact central position of a rod in a tube (true running machine). This showed a deviation of 0.09 mm, which corresponds to the maximal achievable centricity of the rods in the centring device.

The interfaces of 10 rods per alloy and surface were tested 'dry' (i.e., at room temperature and 50% relative humidity) and of 10 rods per alloy and surface 'wet' after immersion in physiological saline solution at 37° C for 60 days.

Push-out tests (Zwick Machine 1488) were carried out with a constant deformation speed of 1 mm/min. Simultaneously, a load-displacement curve was recorded (Fig. 4). The direction of the push-out tests for the rods was from proximal to distal. A straight insertion of the test tube into the push-out machine was ensured by clean-cut distal tube ends and removal of the extruding cement after the end of the cementing process. The maximal load was converted to an interface shear strength using the following formula:

$$\text{Shear strength } \tau \text{ (MPa)} = Fc/2\pi rh$$

where Fc = maximal load (N), r = radius of the rod (mm), h = interface height (mm).

For the microscopic analysis, cylindrical and tapered rods were implanted under room conditions. Six 6-mm cylindrical slices from each surface type were produced by use of a circular carbide saw (Accutom Struers). Subsequent rough grinding (granulation 340), cleaning with ultrasound (Bandelin Souvrex RK 100) and smooth grinding (granulation 600) and again final cleaning in an ultrasound bath prepared the rods for further testing. The cross-sections were analysed under 6.3-fold magnification (Macroscop Wild M420, × 1.25) and documented photographically. The extent of the gap formation between implant and cement was defined as the total of all sections with a gap formation in degrees of the rod circumference. The gap size (μm) between cement and metal was determined with an object micrometer under 200-fold magnification (Zwick Hardness Testing Machine 3213). The extent of the porosity was determined as the area of pores in percentage of the total area. The pores were counted in 6 areas surrounding the implant, each area measuring 1 × 1 cm. The average size of the pores (μm) was studied with the help of the hardness testing machine.

Because of our experience with the shear strength results of the cylindrical rods at the end of our experiments, we started an additional test series with two CoCrMo tapered rods for each surface under 'dry' conditions to see whether the geometry of the implant has an influence on the interface strength. The tapered rods were 60 mm long, with the upper diameter being 10 mm and the lower diameter 8 mm. The overall diameter was reduced over 45 mm. The direction of the push-out tests for the tapered rods was from distal to proximal.

In a second additional series, we tested whether a higher shear strength of the cement-metal interface could be achieved by increasing the pressure in the tube system under 'dry' conditions. Therefore, 5 CoCrMo rods (R_t 60 μm) were implanted, and the tube length was doubled. As in the previous series, the entire tube was filled up with bone cement, and thus, the interface length was doubled as well. The centring device was modified by two pins connected by a metal plate, in order to seal the distal end of the tube.

Results

Under dry conditions, polished and smooth surfaces showed only low shear strengths. The best results of CoCrMo rods were achieved by using surfaces with a roughness (R_t) of 20 μm (8.61 MPa); however, an increase in roughness (R_t) up to 60 μm revealed a slight decrease in shear strength (7.8 MPa). A good shear strength value was obtained with PMMA-precoated rods (5.16 MPa). The debonding area of the CoCrMo and PMMA-precoated rods was always localized between the cement and metal. After immersion in saline solution, all CoCrMo rods, except for the PMMA-precoated rods, failed completely.

Table 1 Shear strength of the cement-metal interface under 'dry' and 'wet' conditions (each series with cylindrical rods $n = 10$, first additional series: tapered rods $n = 2$ and second additional series: cylindrical rods $n = 5$, tube length: 58 mm, modified centring device)

Implant metal (R_t)	Shear strength	
	'Dry' condition	'Wet' condition
Ti-6Al-7Nb Ballotini 0.1–0.2 (7 μm)	3.5 ± 3.05	0.01 ± 0.05
Ti-6Al-7Nb Ballotini 0.1–0.2+E440 (12 μm)	18.46 ± 3.06	0.97 ± 0.47
CoCrMo (1 μm, cylindrical)	0.2 ± 0.1	0
CoCrMo (5 μm, cylindrical)	0.38 ± 0.23	0
CoCrMo (20 μm, cylindrical)	8.61 ± 7.78	0
CoCrMo (60 μm, cylindrical)	7.8 ± 6.4	0
CoCrMo (1 μm, tapered)	0.18 ± 0.06	
CoCrMo (5 μm, tapered)	1.93 ± 0.2	
CoCrMo (20 μm, tapered)	9.8 ± 1.2	
CoCrMo (60 μm, tapered)	2.96 ± 0.69	
CoCrMo precoated (27 μm)	5.16 ± 1.17	4.6 ± 1.68
Additional test series:		
CoCrMo (60 μm, cylindrical)	3.59 ± 1.06	

Table 2 Circumference (°) and size of gap formations (μm) at the cement-metal-interface ($n = 6$) under dry conditions

Implant metal (R_t)	Gap circumference (°)	Gap size (μm)
Ti-6Al-7Nb Ballotini 0.1–0.2 (7 μm)	114	8
Ti-6Al-7Nb Ballotini 0.1–0.2+E440 (12 μm)	99	5
CoCrMo (1 μm, cylindrical)	279	1
CoCrMo (5 μm, cylindrical)	115	1
CoCrMo (20 μm, cylindrical)	245	10
CoCrMo (60 μm, cylindrical)	295	16
CoCrMo (1 μm, tapered)	160	rod dropped off the tube
CoCrMo (5 μm, tapered)	275	15
		rod dropped off the tube
CoCrMo (20 μm, tapered)	209	11
CoCrMo (60 μm, tapered)	350	rod dropped off the tube
CoCrMo precoated (27 μm)	26	4

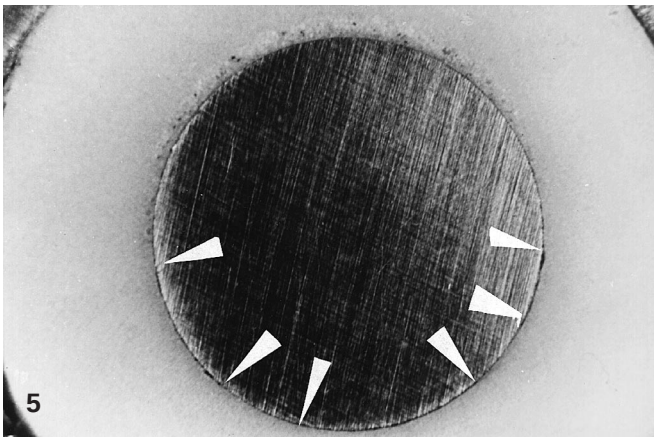

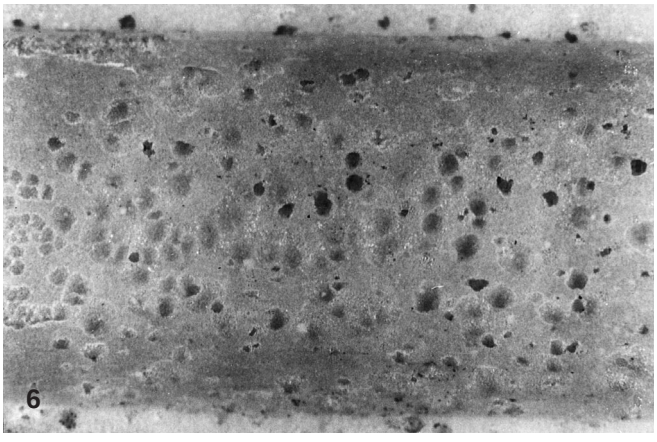

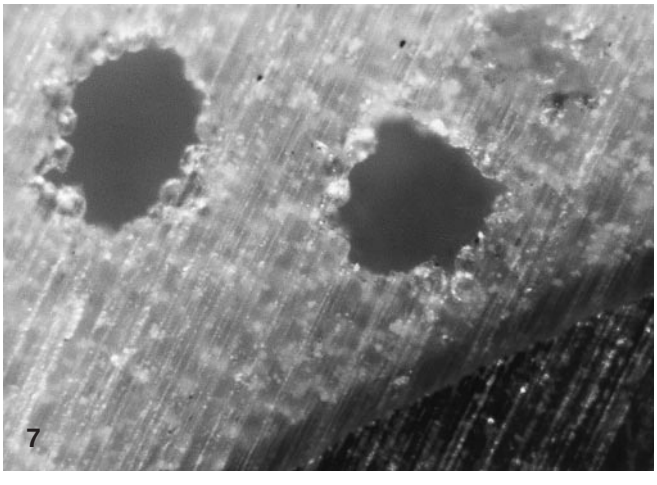

Fig. 5 Cross-section of a rod (CoCrMo R_t 5 µm) with gap formation at the cement-metal interface *(arrows)*

Fig. 6 Longitudinally cut test-tube after the push-out-test demonstrates a porosity adjacent to the interface. The pores rupture partially during the push-out test

Fig. 7 Microscopic sectional view of a precoated rod demonstrates an intact cement-metal interface with pores adjacent to the interface

The shear strength of the PMMA-precoated rods dropped only slightly (Table 1).

The shear strength of the rough Ti-6Al-7Nb rods (R_t 12 µm) was reduced by 94.7%. The smooth titanium rods (R_t 7 µm) failed completely except for one rod. The load-displacement curve illustrates that no strength at all is needed to push the rods out of the test-tube (Fig. 4).

Tapered rods or doubling of the tube length resulted in a similar or lower shear strength in relation to the cement mantle area.

The microscopic analysis showed an average gap formation of 1 µm for CoCrMo rods with a roughness (R_t) of 1 and 5 µm. The gaps were mostly found around the polished surfaces, and this was accompanied by an almost circumferential gap formation (Fig. 5). Rougher CoCrMo surfaces (peak-to-valley height R_t 20 and 60 µm) led to a strikingly wider gap formation, with 10–16 µm on average. Tapered rods revealed similar results, though some rods turned out to be so loose that they had already dropped out of the tubes before the measurements started. In contrast, the average gap formation of the PMMA-precoated rods was only 4 µm (Table 2, Fig. 7).

The cross-sections as well as the longitudinal sections demonstrated pores located close to the interface (Figs. 6 and 7). The average pore diameter was 41 µm (range 5–90 µm) with an average porosity of 12.09%.

Discussion

The experimental design represents the clinical implantation technique including room conditions, although the temperatures of the applied tube materials differed (see below). After using identical cementing techniques, the entrapped air in the tube could leak out distally, which corresponds to the clinical situation of a distal ventilation hole. Excess cement could squeeze out proximally while inserting the test rods.

The experiment was performed with a defined cement mantle thickness of 6 mm, which was chosen according to recommendations of the Exeter prosthesis guidelines (cement mantle thickness 2–6 mm, [6]). Thus, temperature rise, shrinking process due to polymerization, and thermal volume change remained constant.

Clinical observations of the Exeter hip implant from Lee [9] showed that a cement mantle of 5 mm between the medial side of the femoral stem and the neck of the femur provided the best preservation of the calcar. A thick cement layer will require more energy for crack propagation in it, and the effects of stress concentration will be more evident [9].

With regard to the shear strength, the cement mantle thickness is of minor influence, because the failure of the rods was always localized at the cement-mantle interface.

The shear strength under dry conditions points to an optimal surface roughness (R_t) of 20–60 µm for CoCrMo alloys. This statement is only valid for the applied cement type. A further increase in roughness without a lower cement viscosity does not contribute to an improvement of the shear strength. High viscous cement cannot infiltrate sufficiently into the surface roughness and consequently augments additional air being trapped. A large amount of

trapped air decreases the effective contact area between cement and metal.

Thielemann [19] demonstrated a significant improvement of the shear strength by using a low viscosity cement, although this kind of cement is difficult to handle during surgical procedures.

Precoating with a PMMA layer improved the shear strength at the cement-metal interface as well. However, in contrast to results from Stone et al. [18] our obtained shear strength values for PMMA-precoated rods were smaller than those for CoCrMo rods.

Immersion in physiological saline solution has only a minor influence on the shear strength of PMMA-precoated rods, whereas the uncoated rods – independent of their surface roughness – fail completely.

The Ti-6Al-7Nb rods revealed a low remaining shear strength which is insufficient for a stable, long-term bond. Under debonding conditions, titanium alloys show an insufficient corrosion stability. Thus, the implant material characteristics of CoCrMo and titanium must be regarded as the most important difference between the alloys. Due to proved abrasion and corrosion processes with subsequent osteolysis, titanium implants are not recommended for cemented prostheses [20]. Clinical results with aseptic loosening rates of 27.1% 7 years after surgery [13] as well as studies from Agins et al. [1], Salvati et al. [17] and Evans et al. [5] with an average survival rate of 33 months to 4 years confirmed a highly reduced survival rate of cemented titanium implants.

The reason for the loss of bonding is circumferential gaps (average size 1–16 μm) between the PMMA and the implant metal. The gap size depends on the surface roughness of the rod.

The gaps lead to a diminution of the bonding area. Due to their capillary force, the gaps support and accelerate the diffusion of water molecules into the surface.

The permanent dipole moments of the water molecules act as an aggressive medium for the cement-metal bond. Hydrolysis of the initial good bonding stability between metal oxide and carbon and subsequent loss of mechanical stability occur, as the hydrolyzed bondings cannot resist further stress [16]. The remaining mechanical interlocked areas between cement and metal are unable to withstand a measurable shear strength, as proved by our results.

The reason for the gap formation appears to be the trapped air. This assumption is emphasized by the varying degree of the gaps, depending on the surface roughness. This mechanism might also be supported by the shrinking process PMMA undergoes (see below).

The gap formation found in most of the rods at the cement-metal interface led at the end of the experiments to the question of whether a tapered implant design – corresponding to the common shape of an implant – could optimize the situation. It might be possible that air entrapment could be reduced due to an even immersion of the prosthesis in the cement. Therefore, tapered rods were tested in addition to the basic series. However, the results indicated no improvement of the interface strength for a tapered macro design.

Even further pressurization of the system through enlargement of the contact area by doubling the tube length did not lead to an increase of the shear strength. The rather constant shear strength of the PMMA-precoated rods derives from the obviously reduced gap formation as well as from the chemical bond between the cement mantle and precoat which cannot be weakened by water molecules. The smaller amount of gap formation might be caused by a chemical bond.

Other authors [2, 10] confirmed a considerable reduction of the shear strength stability under physiological conditions compared to the ‘dry’ situation. Ahmed et al. [2] observed a significant reduction of the interface stability by a factor of 2.8. Lin et al. [10] proved a more than 2-fold reduction of the interface stability. Davies et al. [4] showed a 1.3-fold reduction of the cement-metal interface stability during the first 18 h of saline immersion.

In contrast to the above quoted results, Thielemann [19] reported shear strength values of 13 MPa for CoCrMo rods, peak-to-valley height R_t 17 μm, and comparable methods after 30 days of saline immersion. Differences from our experiments included the good heat-conductive aluminum as tube material and a cement mantle thickness of 3 mm.

Our own preliminary experiments with aluminum tubes indicate that better results can be achieved with a similar experimental design. In our opinion, the explanation is the change in the outside temperature of the cement mantle. Depending on the temperature gradient, polymerization begins at the outer or inner side of the cement mantle after filling the cement into the tube: With a relative warmer outside, polymerization starts on the outside and induces a shrinkage of the cement away from the implant. Consequently, an opposite situation will lead to a shrinkage of the cement onto the implant.

In vivo, the polymerization process begins at the side of the bone, which represents body temperature, and thus the cement shrinks away from the implant [3]. The occurrence of an interfacial porosity [7] at the cement-metal interface is promoted by the shrinkage of the cement away from the implant and might be eliminated by a reversal of the temperature gradient, e.g. preheating of the stem in vivo [3].

In this study, the observed porosity adjacent to the interface (Fig. 6) resembles the in vivo situation [7] and emphasizes, corresponding to Bishop et al. [3], that a cement shrinking process away from our implants occurred. According to our microscopic observations, the pores rupture partially during the push-out tests but do not have any connection with the observed gap formations. Macroscopic inspection of a longitudinally cut tube after a push-out test showed open pores. Histological analysis of cross-sections revealed a pore-free cement bridge of 100–200 μm between the cement-metal interface and the pores. In a few cases, this distance was decreased to 50 μm (Fig. 7).

Postmortem analyses and clinical results proved the loss of bonding at the prosthesis-cement interface in vivo [8, 15] and confirm our experimental results.

Aside from the PMMA precoating, it is impossible to achieve a sufficient stability of the cement-metal interface

with current techniques. The following are further goals for study:

– Application and further development of PMMA-precoating; experiments to obtain a better adhesion between PMMA and other implant surfaces to eliminate the main weak link;
– Direct influence on the polymerization process to achieve a cement shrinkage towards the implant, e.g., preheating of the stem;
– Abandonment of a stable bond by favoring a primarily sliding interface with a maximally smooth metal surface in order to avoid unnecessary wear. The direct comparison between polished and grit-blasted prosthesis stems over 8 years confirms this concept [11];
– Usage of adhesive surface precoats (for example, Silicoater technique) to obtain an optimized bond between implant surface and cement.

Acknowledgements We would like to thank Zimmer UK, Dr. G. Bensmann, GB Implantattechnologie, Essen, Germany, and Keramed, Germany, for providing the test rods, E. Merck, Darmstadt, Germany, for cement and Dr. G. Bensmann for technical assistance.

References

1. Agins HJ, Alcock NW, Bansal M, Salvati EA, Wilson PD Jr, Pellicci PM, Bullough PG (1988) Metallic wear in failed titanium-alloy total hip replacements: a histological and quantitative analysis. J Bone Joint Surg [Am] 70:347–356
2. Ahmed AM, Raab S, Miller JE (1984) Metal/Cement interface strength in cemented stem fixation. J Orthop Res 2:105–117
3. Bishop NE, Ferguson S, Tepic S (1996) Porosity reduction in bone cement at the cement-stem interface. J Bone Joint Surg [Br] 78:349–356
4. Davies JP, Harris WH (1994) Tensile bonding strength of the cement prosthesis interface. Orthopedics 17:171–173
5. Evans BG, Salvati EA, Huo MH, Huk OL (1993) The rationale for cemented total hip arthroplasty. Orthop Clin North Am 24:599–610
6. Howmedica International (1993) Bewährte Technik für ein sicheres Leben. Exeter das Total-Hüftsystem. Off print (Prospects), Howmedica, Germany
7. James SP, Schmalzried TP, McGarry FJ, Harris WH (1993) Extensive porosity at the cement-femoral prosthesis interface: a preliminary study. J Biomed Mater Res 27:71–78
8. Jasty M, Maloney WJ, Bragdon CR, O'Connor DO, Haire T, Harris WH (1991) The initiation of failure in cemented femoral components of hip arthroplasties. J Bone Joint Surg [Br] 73:551–558
9. Lee AJ (1987) The effect of mixing technique and surgical technique on the properties of bone cement. In: Willert HG, Buchhorn G (eds) Aktuelle Probleme in Chirurgie und Orthopädie 31. Knochenzement. Huber Verlag, Bern
10. Lin ST, Hawkins MT, Parr JE (1995) PMMA precoating technology. Off print (Prospects), Zimmer, USA
11. Malchau H, Herberts T (1996) Prognosis of total hip replacement – a revision-risk study of 134056 primary operations. Presented at 63rd annual meeting of the American Academy of Orthopaedic Surgeons, Atlanta, February 22–26
12. Manley MT, Stern LS (1985) The load carrying and fatigue properties of the stem-cement interface with smooth and porous coated femoral components. J Biomed Mater Res 19:563–575
13. Martell JM, Pierson RH, Sheinkop MB, Galante JO (1990) Results of primary total hip reconstruction with cemented titanium total hip arthroplasty. Minimum four year results. Presented at 57th annual meeting of the American Academy of Orthopaedic Surgeons, New Orleans, February 8–13
14. Mohler CG, Callaghan JJ, Collis DK, Johnston RS (1995) Early loosening of the femoral component at the cement-prosthesis interface after total hip replacement. J Bone Joint Surg [Am] 77:1315–1322
15. Müller RT, Heger I, Oldenburg M (1997) The mechanism of loosening in cemented hip prostheses determined from long-term results. Arch Orthop Trauma Surg 116:41–45
16. Musil R, Tiller HJ (1989) Der Kunststoff-Metall-Verbund in der zahnärztlichen Prothetik. Barth, Leipzig
17. Salvati EA, Betts F, Doty SB (1993) Particulate metallic debris in cemented total hip arthroplasty. Clin Orthop 293:160–173
18. Stone MH, Wilkinson R, Stother IG (1989) Some factors affecting the strength of the cement-metal interface. J Bone Joint Surg [Br] 71:217–221
19. Thielemann F (1994) Experimentelle Untersuchungen zur Haftfestigkeit der Grenzfläche zwischen Implantat und Knochenzement. Promotionalthesis, Universitätsklinikum 'Carl Gustav Carus' der Technischen Universität, Dresden
20. Willert HG, Brobäck LG, Buchhorn GH, Ing D, Jensen PH, Köster G, Lang I, Ochsner P, Schenk R (1996) Crevice corrosion of cemented titanium alloy stems in total hip replacements. Clin Orthop 333:51–75